ELSEVIER

Journal of Nuclear Materials 244 (1997) 205–211

journal of nuclear materials

Total displacement functions for SiC

W.J. Weber [a,*], R.E. Williford [a], K.E. Sickafus [b]

[a] *Pacific Northwest National Laboratory, P.O. Box 999, Richland, WA 99352, USA*
[b] *Materials Science and Technology Division, Los Alamos National Laboratory, Los Alamos, NM 87545, USA*

Received 5 February 1996; accepted 8 August 1996

Abstract

Numerical solutions for the displacement functions in SiC are determined from the coupled integro–differential equations governing the total number of type-j atoms displaced in the collision cascade initiated by a primary knock-on atom (PKA) of type-i and energy E. Atomic scattering cross sections based on either the inverse power law screening potentials or the Ziegler, Biersack, and Littmark (ZBL) universal screening potential are used in the calculation of the displacement functions. The electronic stopping powers used in the calculations are either derived from the LSS and Bethe–Bloch theories or generated from the SRIM-96 electronic stopping power data base. The displacement functions determined using LSS/Bethe–Bloch electronic stopping powers are 25 to 100% larger than the displacement functions determined using the electronic stopping powers generated by SRIM-96. The total number of displaced atoms determined numerically for each PKA type, based on ZBL scattering cross sections and SRIM-96 electronic stopping powers, is in excellent agreement, over the entire range of PKA energies (10 eV to 10 MeV), with the total number of displacements determined by full cascade Monte Carlo simulations using the TRIM code in SRIM-96.

1. Introduction

Due to the high thermal conductivity, high-temperature stability, chemical inertness and small neutron capture cross-section of silicon carbide (SiC), there is increasing interest in SiC based materials for nuclear applications. SiC composites are proposed as low-activation structural components in fusion reactor systems, and SiC is also proposed as an inert host matrix for the burnup of excess weapons plutonium in nuclear reactors or accelerator-based neutron sources. The understanding of irradiation damage in SiC (and other materials) involves both neutron-irradiation studies and ion-beam irradiation studies. Comparison and interpretation of the results from these different experiments involve calculating the total displacement damage under each given set of irradiation conditions.

For neutron irradiations of polyatomic materials, the total displacement damage is determined by integrating the calculated neutron displacement cross-sections over the neutron energy spectrum for the given irradiation. The neutron displacement cross-sections are generally determined using a computer program, such as the SPECOMP code developed by Greenwood [1,2], that integrates the displacement functions for all possible combinations of primary knock-on atoms (PKAs) and matrix atoms over libraries of PKA spectra for most elements. Huang and Ghoniem [3] have described in detail the determination of the displacement functions for SiC and the integration of the total displacement functions over the neutron elastic scattering cross sections for Si and C to yield the neutron displacement cross sections associated with elastic neutron scattering in SiC. The displacement functions for polyatomic materials are generally determined by numerical solution of the coupled integro–differential equations defined by Parkin and Coulter [4–6], as was the case in the study of Huang and Ghoniem [3]. These equations determine the net or total number of displaced atoms; however, they do not determine the spatial distribution of the displaced atoms.

For ion-beam irradiation studies, the Monte Carlo computer code TRIM [7–9] (TRansport of Ions in Matter) is

* Corresponding author. Tel.: +1-509 375 2299; fax: +1-509 375 2186; e-mail: wj_weber@pnl.gov.

PII S0022-3115(96)00738-6

widely used to simulate the slowing down and scattering of energetic ions. By following a large number of individual ions, TRIM determines the implanted-ion distributions and the spatial distribution of displaced atoms in monoatomic, polyatomic, and multilayered materials. The Monte Carlo approach provides a more rigorous treatment of the elastic scattering, and current versions of TRIM use the Ziegler, Biersack, and Littmark (ZBL) universal screening potential [8,9] to calculate the scattering angle and energy transfer that results from each binary nuclear collision. An additional feature of the TRIM code is that the results from neutron transport code calculations (position and recoil statistics for each collision atom) can be used to generate a TRIM source file that can be used by TRIM (1992 and later versions) to calculate the full recoil cascade and total displacements that occur for each PKA. Thus, TRIM could be used as an alternative or as a complement to codes such as SPECOMP for neutron irradiations.

TRIM-95, the program package that includes TRIM, was originally used in these calculations for SiC [10] and included a significant revision of the data base that is used to generate stopping powers for monoatomic and polyatomic materials. Due to a bug in the stopping power program of TRIM-95, the electronic stopping powers for solid forms of gases (or solids containing gas species) were in error at low energies (by over 200% at energies below 25 eV [11]). In the case of SiC, the TRIM-95 electronic stopping powers for C and Si ions were in error by 100% at the lower energy range of the calculations in this study. This problem has been corrected in the 1996 version of this program package, which has been renamed SRIM (Stopping and Range of Ions in Matter) to distinguish it from the Monte Carlo code TRIM that is also included.

The computational approaches used to determine total displacements in polyatomic materials under neutron irradiation and under ion-beam irradiation are different; however, both approaches assume the binary collision approximation that treats PKA trajectories as a series of two-body collisions. For neutron irradiation of polyatomic materials, numerical solutions of the integro–differential equations of Parkin and Coulter [4–6] determine the displacement functions used to calculate total displacements, and the two-body atomic scattering cross sections used in these calculations are generally approximated by analytical fits to dimensionless scattering functions that are derived for different forms of the screening potential. In the case of ion-beam irradiations of polyatomic materials, more rigorous Monte Carlo methods, generally using TRIM and the ZBL universal potential [8,9], are used to determine the spatial distribution of displaced atoms, as well as the total number of displacements. The Monte Carlo code TRIM follows the trajectories of each incident ion and all recoils. Changes in direction are the result of binary nuclear collisions that are governed by the classical equations of motion for a particle in a central-force field [9,12] defined by the interatomic screening potential (i.e., the ZBL potential). Energy is lost in discrete amounts in the nuclear collisions and continuously from electronic interactions (i.e., the electronic stopping power). The trajectories for a large number of incident ions or PKAs must be calculated using TRIM to achieve high statistics, which can require long computation time.

The major differences in these two approaches to determining total displacements are the method of solution (analytical versus Monte Carlo) and the choice of interatomic screening potentials (or derived atomic scattering cross sections) and electronic stopping powers. If the total number of displaced atoms calculated by the two approaches differ significantly, there will be a systematic error when comparing (on the basis of total displaced atoms) neutron-irradiation results with the results from ion-beam-irradiation studies. The objective of the present paper is to determine the total displacement functions for SiC by solving numerically the coupled integro–differential equations defined by Parkin and Coulter [4–6], using different atomic scattering cross sections and electronic stopping powers, and to compare the results with the total number of displaced atoms determined by full cascade Monte Carlo simulations using the TRIM code in SRIM-96.

2. Theory

2.1. Net displacement function

The displacement function, $\nu_{ij}(E)$, for polyatomic materials is the average number of type-j atoms displaced in a collision cascade initiated by a type-i PKA of energy E and is generally described by an integro–differential equation originally defined by Parkin and Coulter [4–6]. In this paper, the equivalent notation of Huang and Ghoniem [3] for describing $\nu_{ij}(E)$ is followed, with the integro–differential equation given by

$$S_i(E)\frac{\mathrm{d}\nu_{ij}(E)}{\mathrm{d}E} = \sum_k f_k \int_0^{\Lambda_{ik}E} \mathrm{d}T \frac{\mathrm{d}\sigma_{ik}(E,T)}{\mathrm{d}T} \times \Big(\Gamma(T - E_{kd}) \big[\delta_{kj} + \nu_{kj}(T) \big] + \Gamma(E - T - E_{jd}/\Lambda_{ij})\, \nu_{ij}(E - T) - \nu_{ij}(E) \Big) \qquad (1)$$

where $S_i(E)$ is the electronic stopping power of type i atoms in the polyatomic material, f_k is the atomic fraction of type k atoms in the material, Λ_{ik} is the kinematic energy transfer efficiency between atoms of type i and k, $\Gamma(x)$ is the step function, δ_{kj} is the Kronecker delta function, E_{kd} is the displacement threshold energy for atoms of type k in the material, and σ_{ik} (E, T) is the atomic scattering cross section of type i atoms with energy E that transfers energy T to atoms of type k. The kine-

matic energy transfer efficiency, A_{ik}, in Eq. (1) is the maximum fraction of energy that can be transferred from an atom of type i to an atom of type k and is given by

$$A_{ik} = \frac{4A_iA_k}{(A_i + A_k)^2} \tag{2}$$

where A_i and A_k are the atomic weights, respectively. Since Eq. (1) for $\nu_{ij}(E)$ also contains $\nu_{kj}(E)$ terms, it is coupled to equivalent equations for each type-k PKA ($k \neq i$). For a two-component material, as in the present study, there are two coupled integro–differential equations for each PKA of type i, one for $\nu_{ij}(E)$ and one for $\nu_{jj}(E)$, that must be solved simultaneously.

The coupled integro–differential equations represented by Eq. (1) can be solved simultaneously by numerical methods. A computer code was developed to numerically integrate these equations for materials containing several atom types and for different forms of the atomic scattering cross sections and electronic stopping powers. Analogous to the work of Huang and Ghoniem [3], the basic method of numerical integration was a fifth order Runge–Kutta [13] integration that maintained an accuracy of 0.001% by automatic adjustment of step size. The integrations were subject to the boundary condition that $\nu_{ij}(E) = 0$ for $E \leq E_{jd}/A_{ij}$. The computer code was written in Fortran and runs on a Power MacIntosh computer. Typical computations for energies up to 10^7 eV required less than 5 min to run with a 66 MHz processor.

2.2. Electronic stopping powers

The electronic stopping power, $S_i(E)$, of type-i atoms in a polyatomic material can be estimated from Bragg's Rule [14], which states that $S_i(E)$ is related to the linear sum, over all atom types, of electronic stopping powers, $S_k(E)$, of type-i atoms in monoatomic type-k targets. According to Bragg's Rule, $S_i(E)$, with units of eV cm^2/atom, is given by the expression:

$$S_i(E) = \sum_k f_k S_{ik}(E) \tag{3}$$

where f_k is the atomic fraction. The stopping powers, $S_{ik}(E)$, for different materials can be obtained from experimental data, the tables of Northcliffe and Schilling [15], the electronic stopping theories of Lindhard, Scharff and Schiøtt (LSS) [16,17] and Bethe–Bloch [18,19], or the output of SRIM-96 (or previous TRIM versions). Baglin and Ziegler [20] have shown that for 2.0 MeV He ions the measured stopping powers in single crystal (3C and 6H) and polycrystalline SiC are within 2% of the stopping power predicted by Bragg's Rule from the measured stopping powers in silicon and carbon. In the studies of Parkin and Coulter [4–6], Bragg's Rule coupled with LSS electronic stopping powers was used to define the stopping powers for polyatomic materials. Huang and Ghoniem [3] in their study of displacement functions in SiC also employed Bragg's Rule; however, they used the LSS theory to calculate the electronic stopping power at low to intermediate energies and the Bethe–Bloch theory at high energies. In order to cover the entire energy range and to provide a realistically smooth transition, Huang and Ghoniem bridged the LSS and Bethe–Bloch stopping powers according to the procedure outlined by Biersack and Haggmark [21]. As an integral part of the numerical code developed under this study, both the LSS and Bethe–Bloch electronic stopping powers for polyatomic materials are calculated according to Eq. (3) and then bridged using the Biersack and Haggmark method [21] to provide a smooth transition. The calculated LSS, Bethe–Bloch, and bridged LSS/Bethe–Bloch electronic stopping powers for C and Si ions in SiC are shown in Figs. 1 and 2, respectively.

The electronic stopping power calculated by SRIM-96 for 2.0 MeV He ions in SiC is in excellent agreement (within 2.5%) with the experimental values [20]. For ions other than H and He, SRIM calculates electronic stopping powers by scaling proton electronic stopping powers, as described by Ziegler [9]. The electronic stopping powers calculated by SRIM-96 for C ions in SiC (Fig. 1) and used in the TRIM calculations are larger than the bridged LSS/Bethe–Bloch electronic stopping powers over the entire energy range of interest (10^2 to 10^7 eV); this difference will affect the calculated displacement functions, as described below. The SRIM-96 electronic stopping powers for Si ions in SiC (Fig. 2) that are used in TRIM are in good agreement with the LSS/Bethe–Bloch stopping powers for energies below 1 MeV. Above 1 MeV, the SRIM-96 stopping powers for Si ions in SiC are larger than the LSS/Bethe–Bloch stopping powers; however, since the atomic scattering cross sections are very small at these energies, the differences in electronic stopping powers for Si ions should have only a small effect on the numerical solutions. In order to compare the effects of

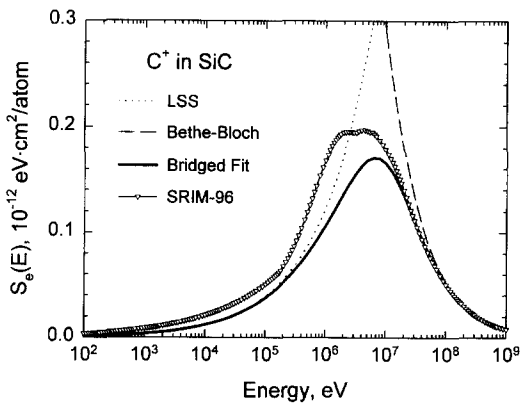

Fig. 1. Calculated electronic stopping powers for C ions in SiC.

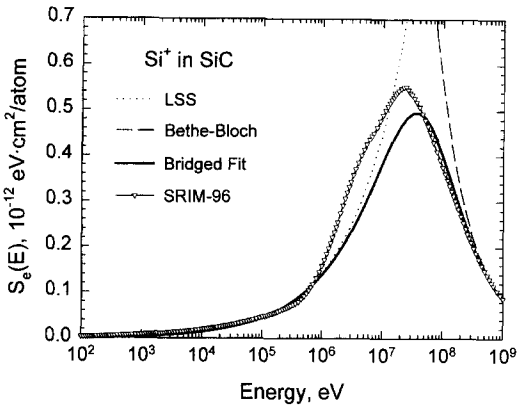

Fig. 2. Calculated electronic stopping powers for Si ions in SiC.

the different stopping powers, the SRIM-96 electronic stopping powers for SiC have been tabulated and used as a data source file in the numerical code to determine the displacement functions. Other values for the electronic stopping powers (theoretical, experimental, etc.) also could be tabulated into a data source file and used in the numerical calculations.

2.3. Atomic scattering cross sections

The atomic scattering cross section in Eq. (1) is dependent on the form of the screened potential used to describe the forces between the interacting atoms. Winterbon, Sigmund and Sanders (WSS) [22] have shown that the atomic scattering cross section based on the Thomas–Fermi potential can be approximated by matching scattering cross sections based on inverse power law potentials. A modified form of the WSS power law cross section [23] was used by Huang and Ghoniem [3] to calculate the displacement functions for SiC. The modified WSS atomic scattering cross section for SiC, as defined by Huang and Ghoniem [3], was used initially in the present study, as it allowed direct comparison to their results during development of the displacement function code. Since the ZBL (Ziegler, Biersack, Littmark) universal potential [8,9] is used by SRIM–96 in the Monte Carlo (TRIM) calculation of atomic scattering events, an analytical approximation to the atomic scattering cross section, based on the ZBL universal potential [8], is used in all other calculations of the displacement functions for SiC. The ZBL differential atomic scattering cross section, in terms of the LSS reduced units, can be expressed as

$$\mathrm{d}\sigma_{ik}(E,T) = \frac{\pi a_u^2}{2}\frac{f(t^{1/2})}{t^{3/2}}\,\mathrm{d}t \tag{4}$$

where a_u is the ZBL universal screening length, t is the dimensionless collision parameter, and $f(t^{1/2})$ is the scattering function that is defined by the ZBL universal potential. The parameters a_u and t are given by

$$a_u = \frac{0.8854 a_o}{\left(Z_i^{0.23} + Z_k^{0.23}\right)} \tag{5}$$

and

$$t = ET\frac{A_k}{A_i}\frac{a_u^2}{4Z_i^2Z_k^2e^4} \tag{6}$$

where a_o is the Bohr radius, Z_i and Z_k are the atomic numbers, and A_i and A_k are the atomic weights of atoms of type i and k, respectively. An analytical approximation to the scattering function, which was originally derived by Winterbon et al. [22] for a Thomas–Fermi potential and recently fitted by Nastasi, Mayer and Hirvonen [25] for the ZBL universal potential, is given by

$$f(t^{1/2}) = \lambda t^{(1/2-m)}\left[1 + (2\lambda t^{(1-m)})^q\right]^{-1/q} \tag{7}$$

where the fitting parameters λ, m, and q are given by the values 5.012, 0.203, and 0.414, respectively, for the ZBL universal potential. (For the Thomas–Fermi potential, λ, m, and q are given by the values 1.309, 1/3, and 2/3, respectively [22].)

2.4. Displacement threshold energies

Solutions to the coupled integro–differential equations are dependent on the displacement threshold energies, E_{jd}, used. The displacement threshold energies in SiC are controversial; however, in the comparison of the computational methods in this paper, the exact values are less important than the consistent use of the same values in all calculations. In the present study, the displacement threshold energies, E_d(C) and E_d(Si), assumed for C and Si in SiC are 16.3 and 92.6 eV, respectively. These values were determined using molecular dynamics simulation techniques [24] and are the same values used in the study of Huang and Ghoniem [3]. Other values can be easily incorporated into the calculations to evaluate the effects on damage stoichiometry or to determine displacement cross sections once the displacement threshold energies are better defined for SiC.

3. Results and discussion

3.1. Numerical solutions

Numerical solutions to Eq. (1) for the displacement functions, $\nu_{ij}(E)$, in SiC have been calculated using the modified WSS power law cross sections [3] and the LSS/Bethe–Bloch electronic stopping powers (Figs. 1 and 2). The results, which are shown in Fig. 3, are about a factor of two lower than the results previously calculated by Huang and Ghoniem [3]. The reason for this difference

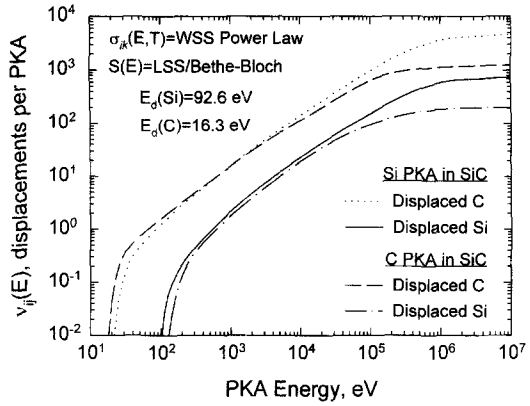

Fig. 3. Displacement functions, $\nu_{ij}(E)$, in SiC calculated using the bridged LSS/Bethe–Bloch electronic stopping powers (Figs. 1–2) and the modified WSS power law cross sections [3].

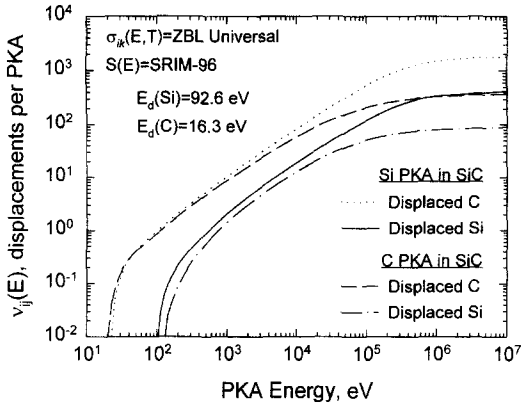

Fig. 5. Displacement functions, $\nu_{ij}(E)$, in SiC calculated using the SRIM-96 electronic stopping powers (Figs. 1–2) and the ZBL atomic scattering cross sections [8].

is not known. In Fig. 4, numerical solutions for $\nu_{ij}(E)$ in SiC based on using the ZBL scattering cross sections, defined by Eq. (4), and the LSS/Bethe–Bloch electronic stopping powers are shown. Numerical solutions based on using the ZBL scattering cross sections and the electronic stopping powers generated by SRIM-96 are shown in Fig. 5. (Note: numerical calculations using cross sections based on Eq. (7) for the Thomas–Fermi potential are within 20% of the ZBL results over the entire energy range considered.)

The results in Figs. 3–5 show that $\nu_{ij}(E)$ goes to zero at E_{jd}/Λ_{ij} in accordance with the boundary conditions, with $\nu_{ij}(E)$ for like atoms (i.e., $i=j$) going to zero at E_{jd}, since $\Lambda_{ij}=1$ under this condition. The results also show that the number of C atoms displaced by each PKA type is about a factor of 6 larger than the number of displaced Si atoms due to the lower displacement threshold energy used for C (16.3 eV) than used for Si (92.6 eV) in these calculations. At energies above about 0.2 MeV, the displacement functions all begin to saturate as the atomic scattering cross sections go to zero.

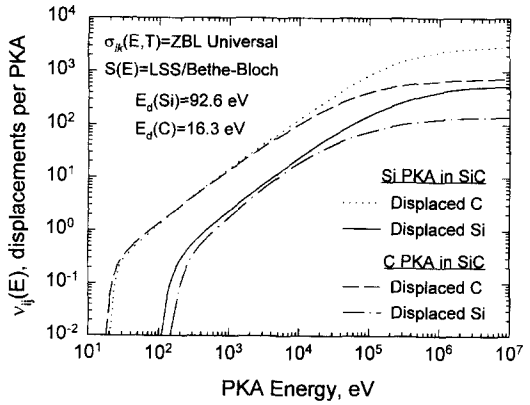

Fig. 4. Displacement functions, $\nu_{ij}(E)$, in SiC calculated using the bridged LSS/Bethe–Bloch electronic stopping powers (Figs. 1–2) and the ZBL atomic scattering cross sections [8].

For the two cases where the LSS/Bethe–Bloch electronic stopping powers are used in the numerical calculations, the displacement functions based on the ZBL scattering cross sections (Fig. 4) are indistinguishable from the results based on the modified WSS power law cross sections (Fig. 3) for C PKA energies below 20 keV and for Si PKA energies below 100 keV. This result indicates a negligible effect in this energy range from the differences in the approximations to the scattering cross sections. At higher energies, the displacement functions for the ZBL scattering cross sections are about 40% lower than the results for the modified WSS cross sections; this is not surprising, since the ZBL scattering cross sections decrease more rapidly at high energies than the WSS power law cross sections.

Where the ZBL atomic scattering cross sections are used in the numerical calculations, the displacement functions (Fig. 4) based on LSS/Bethe–Bloch stopping powers are slightly larger than the displacement functions (Fig. 5) based on SRIM-96 electronic stopping powers over the entire energy range of the calculations. As discussed above, the electronic stopping powers for Si in SiC are in good agreement below 1 MeV (Fig. 2), and above this energy, the effects of any differences in electronic stopping powers should be negligible. Consequently, the differences between the results in Fig. 4 and the results in Fig. 5, which range from $< 25\%$ for Si PKAs and Si displacements to 100% for C PKAs and C displacements, are due to the larger values of the SRIM-96 electronic stopping power for C in SiC relative to the LSS/Bethe–Bloch stopping power (Fig. 1). The largest difference in the displacement functions occurs above 0.1 MeV, where the differences in electronic stopping powers for C in SiC are greatest. Above 1 MeV, the atomic scattering cross sections for the ZBL potential decrease rapidly, and the effects of differences in the electronic stopping powers saturate, with no additional effects discernable.

3.2. Monte Carlo calculations

Monte Carlo calculations using TRIM do not include each $\nu_{ij}(E)$ specifically in the output; instead the sum of the total displacements, including replaced atoms, $(\nu_{ii}(E) + \nu_{ij}(E))$ for each incident ion of energy E is provided. In order to compare the two methods of calculation, the numerical results in Figs. 3–5 are summed for each PKA type, and the results are shown in Figs. 6 and 7 for C and Si PKAs, respectively, along with the results of full cascade Monte Carlo calculations using the TRIM code in SRIM-96. A minimum of ten thousand ions were calculated for each value of ion energy to obtain good statistics. The differences in the numerical solutions, discussed above, are more clearly seen in the comparison of results in Figs. 6 and 7. A significant effect of the differences in atomic scattering cross sections is observed only at the higher energies (> 20 keV for C ions and > 100 keV for Si ions) and, as noted, is due to the more rapid decrease of the ZBL scattering cross sections at these energies.

The effect of using the SRIM-96 electronic stopping powers is to decrease the calculated number of total displaced atoms relative to those calculated using the LSS/Bethe–Bloch electronic stopping powers. The SRIM calculations of electronic stopping powers are based on recent theoretical developments and updated data bases. The accuracy of the LSS electronic stopping powers, however, is only about a factor of 2, since the theory does not allow for any shell structure in the target atoms [9]. Consequently, the more accurate SRIM electronic stopping powers should be considered for use in neutron damage calculations, particularly if comparisons with ion-beam results are to be made.

The total number of displaced atoms determined numerically for both C and Si PKAs (Figs. 6 and 7), based on ZBL atomic scattering cross sections and SRIM-96 electronic stopping powers, is in excellent agreement, over the entire range of PKA energies (10 eV to 10 MeV), with the total number of displacements determined by rigorous Monte Carlo simulations using the TRIM code in SRIM-96. These results confirm the validity of the numerical solutions. Thus, numerical determinations of neutron displacement functions using the ZBL scattering cross sections and SRIM electronic stopping powers are not only more accurate for polyatomic materials, such as SiC, but also allow the comparison of neutron and ion-beam irradiation results to be made with greater confidence.

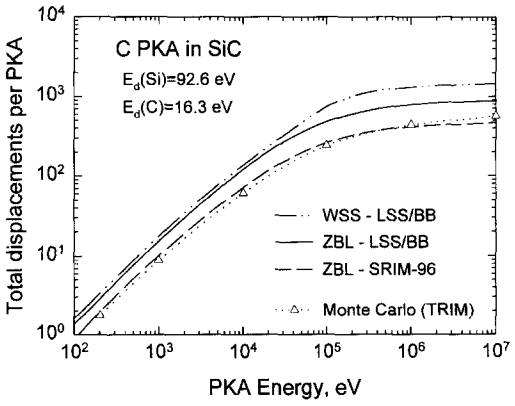

Fig. 6. Total number of displaced atoms for a C PKA of energy E in SiC. Comparison of numerical solutions to Eq. (1), using WSS power law or ZBL universal scattering cross sections and LSS/Bethe–Bloch (LSS/BB) or SRIM-96 electronic stopping powers, and results of Monte Carlo calculations using TRIM in SRIM-96.

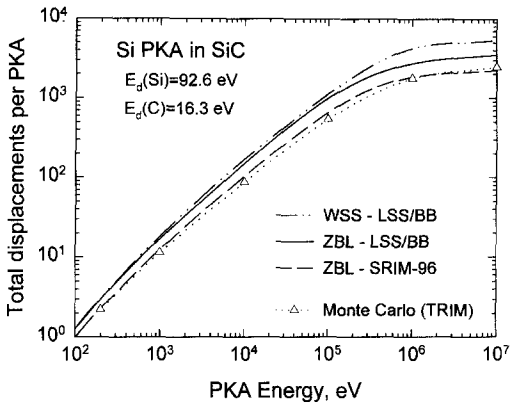

Fig. 7. Total number displaced atoms for a Si PKA of energy E in SiC. Comparison of numerical solutions to Eq. (1), using WSS power law or ZBL universal scattering cross sections and LSS/Bethe-Bloch (LSS/BB) or SRIM-96 electronic stopping powers, and results of Monte Carlo calculations using TRIM in SRIM-96.

4. Summary

The differences in the ZBL and WSS power law scattering cross sections have a small effect on the total displacement functions for C PKA energies below 20 keV and for Si PKA energies below 100 keV. At higher energies, displacement functions based on the ZBL scattering cross sections will tend to be up to 40% less than the displacement functions calculated using the WSS power law cross sections, due to the more rapid decrease in the ZBL scattering cross sections at these energies.

Differences in the electronic stopping powers have the largest effect on the determination of the total displacement functions in SiC. The electronic stopping powers generated by SRIM-96 for C and Si ions in SiC are considered more accurate. The SRIM-96 electronic stopping powers for C in SiC are larger than the electronic stopping powers calculated by bridging the LSS and Bethe–Bloch stopping powers; the SRIM-96 stopping powers for Si in SiC, however, are in reasonable agreement with the bridged LSS/Bethe–Bloch stopping pow-

ers. The larger electronic stopping powers for C significantly decrease (up to 50%) the total displacement functions. Since most neutron displacement cross sections for materials are based on using LSS or bridged LSS/Bethe–Bloch electronic stopping powers, the results suggest there may be a systematic 25 to 100% difference in calculated dose when comparing neutron-irradiation results on SiC with ion-beam-irradiation results. The differences in calculated dose are greatly reduced if the same electronic stopping powers (and the same atomic scattering cross sections) are used as the basis for calculations of total displacements under both neutron and ion-beam irradiations.

Acknowledgements

This research was supported by the Division of Materials Sciences, Office of Basic Energy Sciences, U.S. Department of Energy under Contract DE-AC06-76RLO 1830 at Pacific Northwest National Laboratory and under Contract W-7405-ENG-36 at Los Alamos National Laboratory.

References

[1] L.R. Greenwood, in: Reactor Dosimetry: Methods, Applications and Standardization, ASTM-STP 1001, eds. H. Ferrar IV and E. Lippincott (American Society for Testing and Materials, Philadelphia, 1989) pp. 596–602.
[2] L.R. Greenwood, J. Nucl. Mater. 216 (1994) 29.
[3] H. Huang and N. Ghoniem, J. Nucl. Mater. 199 (1993) 221.
[4] D.M. Parkin and C.A. Coulter, J. Nucl. Mater. 101 (1981) 261.
[5] D.M. Parkin and C.A. Coulter, J. Nucl. Mater. 103–104 (1981) 1315.
[6] D.M. Parkin and C.A. Coulter, J. Nucl. Mater. 117 (1983) 340.
[7] J.P Biersack and L.G. Haggmark, Nucl. Instrum. Methods 174 (1980) 257.
[8] J.F. Ziegler, J.P. Biersack and U. Littmark, The Stopping and Range of Ions in Solids (Pergamon Press, New York, 1985).
[9] J.F. Ziegler, in: Handbook of Ion Implantation Technology, ed. J.F. Ziegler (North Holland, Amsterdam, 1992) pp. 1–68.
[10] W.J. Weber, R.E. Williford and K.E. Sickafus, presented at the TMS Annual Meeting, Anaheim, CA, February, 1996.
[11] J.F. Ziegler, personal communication.
[12] M.T. Robinson, J. Nucl. Mater. 216 (1994) 1.
[13] W.H. Press, B.P. Flannery, S.A. Teukolsky and W.T. Vetterling, Numerical Recipes (Cambridge University Press, Cambridge, UK, 1986) ch. 15, pp. 554–560.
[14] W.H. Bragg and R. Kleeman, Philos. Mag. 10 (1905) 5318.
[15] L.C. Northcliffe and R.F. Schilling, Nucl. Data Tables A 7 (1970) 233.
[16] J. Lindhard, M. Scharff and H.E. Schiøtt, Mat. Fys. Medd. Dan. Vid. Selsk. 33(14) (1963).
[17] J. Lindhard and M. Scharff, Phys. Rev. 124 (1961) 128.
[18] H.A. Bethe. Ann. Phys. 5 (1930) 325.
[19] F. Bloch, Ann. Phys. 16 (1933) 287.
[20] J.E.E. Baglin and J.F. Ziegler, J. Appl. Phys. 45 (1974) 1413.
[21] J. Biersack and L. Haggmark, Nucl. Instrum. Methods 174 (1980) 257.
[22] K.B. Winterbon, P. Sigmund and J.B. Sanders, Mat. Fys. Medd. Dan. Vid. Selsk. 37(14) (1970).
[23] P. Chou, Ph.D. Thesis at UCLA, May (1986).
[24] A. El-Azab and N.M. Ghoniem, J. Nucl. Mater. 191–194 (192) 1110.
[25] M. Nastasi, J.W. Mayer, J.K. Hirvonen, Ion–Solid Interactions: Fundamentals and Applications (Cambridge University Press, Cambridge, UK, 1996), pp. 98–99.